IEEE/CSC & ESAS European Superconductivity News Forum (ESNF), No. 14, October 2010
The published version of this manuscript appeared in *IEEE Transactions on Applied Superconductivity* **21**, Issue 3, 456 - 460 (2011)

Co-registration of MEG and ULF MRI using a 7 channel low-T_c SQUID system

Per E. Magnelind, John J. Gomez, Andrei N. Matlashov, Tuba Owens, J. Henrik Sandin, Petr L. Volegov, and Michelle A. Espy

***Abstract*—In this paper we report the first co-registered, interleaved measurements of ultra-low field (ULF) magnetic resonance imaging (MRI) and magnetoencephalography (MEG). The measurement system consisted of 7 channels with second-order gradiometers coupled to low transition-temperature superconducting quantum interference devices (SQUIDs). The ULF MRI was acquired at a measurement field of 94 μT after a pre-polarization in a 30 mT field. Our results show that the two modalities can be performed with interleaved measurements. However, due to transients from the walls of the magnetically shielded room a waiting time of more than 3 s had to be introduced between the MRI protocol and the auditory stimulus for the MEG.**

***Index Terms*—magnetoencephalography, microtesla, magnetic resonance imaging.**

I. INTRODUCTION

In human brain imaging, e.g. pre-surgical mapping, it is highly desired to obtain images with high spatial and temporal resolution. However, no single imaging device is capable of producing both a high spatial resolution anatomical image and a high temporal resolution functional image.

During the last couple of years significant efforts have been directed towards magnetic resonance imaging (MRI) in fields comparable to the Earth's field [1]-[12], i.e. microtesla fields, or lower fields. The fields in this range are called ultra-low fields (ULF). Interestingly, the idea of magnetic resonance at microtesla fields is more than 50 years old [13].

In ULF MR it is essential to use pre-polarization to increase the signal-to-noise ratio of the signal from the precessing spins, since the magnetization from the measurement field alone is very small. Even with the present level of pre-polarization the ULF images are not as highly resolved as their high-field counterparts.

By using a 7 channel system equipped with low transition temperature (T_c) Superconducting QUantum Interference Devices (SQUIDs) to perform both ULF MRI and magnetoencephalography (MEG; [14]), it is possible to co-register a lower resolution ULF MR image and an MEG image obtained during one run. Thereby, the MEG data is aligned to the ULF MR image after performing a calibration run with a phantom. The ULF MR image can then be used to align the MEG data onto a high-field MR image.

Recently, our group presented the first brain images obtained by ULF MRI [6]. The MR imaging was combined with an MEG session performed a posteriori. The subject's head was moved in between the MRI run and the MEG run and no reference coils were used to quantify the translation. The main reason for the translation of the head was to improve the coverage of the auditory evoked response.

In this paper, we report interleaved ULF MRI and MEG measurements co-registered in the same system.

II. EXPERIMENTAL

The ULF MRI/MEG system used here is described in detail in, e.g., [5]. In brief, it consists of a helium cryostat with seven wire-wound 2nd order gradiometers, which are coupled to CE2Blue SQUIDs [15] through circuits with SW1 cryo-switches [15]. The gradiometers have a diameter of 37 mm, a baseline of 60 mm, and are positioned with a 45 mm spacing in a hexagonal pattern around one in the center. The corresponding magnetic flux density noise of the sensors are 1.2-2.8 fT/Hz$^{1/2}$.

The MRI fields were generated by copper coils powered by car batteries for low noise performance. A 3D Fourier imaging protocol was used (see Fig. 1) with frequency encoding, $G_x = dB_z/dx = \pm 150$ μT/m, phase encoding, $|G_z| = |dB_z/dz| \leq 140$ μT/m (51 encoding steps) and $|G_y| = |dB_z/dy| \leq 66$ μT/m (9 encoding steps). The resulting voxel size was 3 × 3 × 6 mm^3. The encoding and acquisition times were 28 ms and 56 ms, respectively.

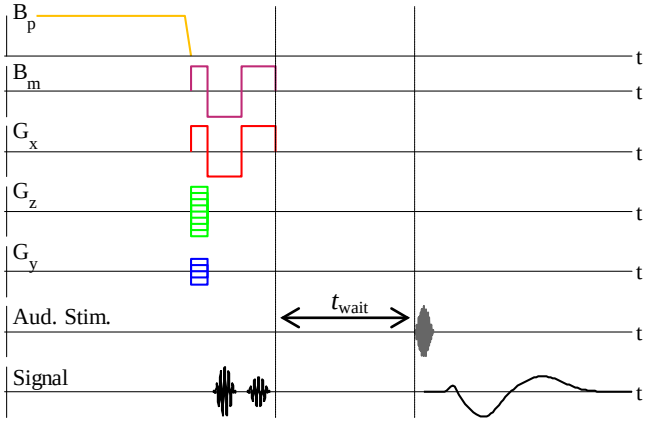

Fig. 1. Pulse sequence for the ULF-MRI and MEG co-registration showing the pre-polarization, the MR imaging protocol, the auditory stimulus, and the measured signals.

Manuscript received 3 August 2010. This work was supported in part by the National Institute of Health through grant 5 R01 EB006456 and the Los Alamos National Laboratory LDRD office through grant 20100097DR.

The authors are with the Los Alamos National Laboratory, Applied Modern Physics Group, P.O. Box 1663, MS-D454, Los Alamos, NM 87545, USA (phone: 505-665-0021; fax: 505-665-4507; e-mail: per@lanl.gov).

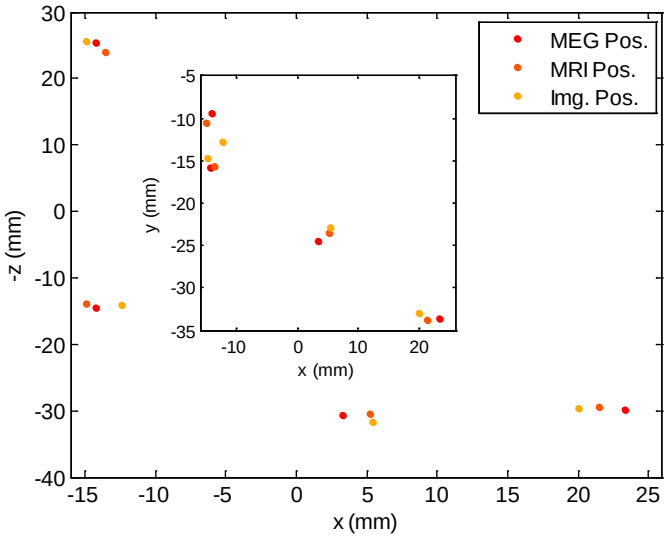

Fig. 2. Coordinates for the vials and coils of the co-registration phantom. The points show the calculated position of the coil from the different modalities, where Img. Pos. comes from a photograph of the phantom.

The pre-polarization coils were cooled by liquid nitrogen. The pre-polarization field, B_p, was ~30 mT and was applied during 1 s. To provide insulation for the subject NanoPore [16] vacuum insulated panels were used in addition to cellfoam panels.

The measurement field, B_m, was 94 μT which corresponds to a Larmor frequency of 4 kHz.

The auditory stimulus consisted of a 68 ms long, single-lobe sinc pulse with a 2 kHz frequency. The wait time, t_{wait}, in between the last step of the MRI protocol and the beginning of the auditory stimulus was 3.3 s. The SQUIDs were turned on 0.7 s before the on-set of the stimulus.

The pulse sequence provides one MEG epoch for each *k*-space point. In the imaging protocol there were 51×9 = 459 points.

Before each run a head localization scheme was employed. First, a swim-cap equipped with small copper coils was put on the subject's head. Second, the position of the individual coils and three fiducial points were mapped using a Polhemus 3Space Fastrak [17]. Third, the subject was positioned inside the measurement system and current was sequentially passed through the coils and the generated magnetic fields were measured by the SQUIDs. Fourth, the coil positions were found by fitting coil positions and orientations to the magnetic field maps.

To get a calibration of the ULF MRI and MEG coordinate systems a phantom with four cylindrical 2 ml water vials and small coils attached to each vial was used. The vials were placed at different heights and with different distances in-between each other. As with the head-localization coils, a Polhemus mapping was carried out and once inside the system current was passed sequentially through the four coils. An MR image was obtained and used to find the translation between the MRI and MEG coordinate systems.

The experiments involving human subjects were approved by the Los Alamos Institutional Review Board and informed consent was obtained from the involved subject.

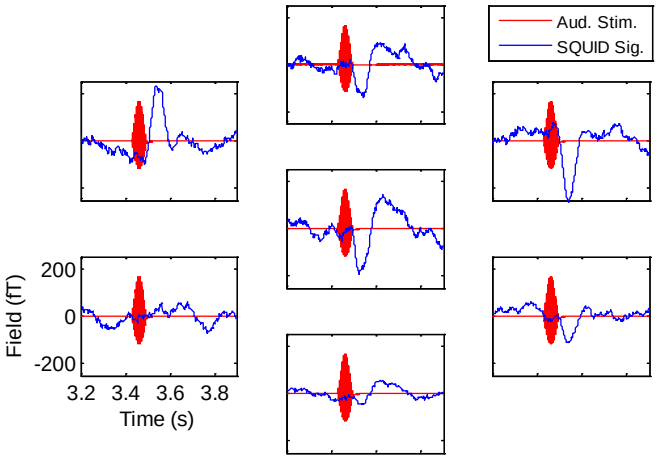

Fig. 3. MEG signals from the 7 channels with the auditory stimulus. The subfigures are arranged in the same arrangement as the channels in the system.

III. Results

We have measured interleaved ULF-MRI and MEG in our 7 channel low-T_c SQUID system. The results are reported below.

A. *Coordinate systems calibration*

Results from the Polhemus mapping, the coil localization, and the MRI are shown in Fig. 2. The points in the figure show the calculated positions of the vials/coils for the different localization methods. The co-registration error was a few millimeters.

B. *Magnetoencephalography*

The MEG epochs without steps in the data (387 out of 459) were averaged for each channel and low-pass filtered at 200 Hz. Fig. 3 shows the MEG data and the auditory stimulus. Peaks of different polarity are visible ~100 ms after the stimulus on-set. These peaks show the N100m response of the auditory cortex. The N100m peak values are shown as a field map overlaid on the subject's head in Fig. 4.

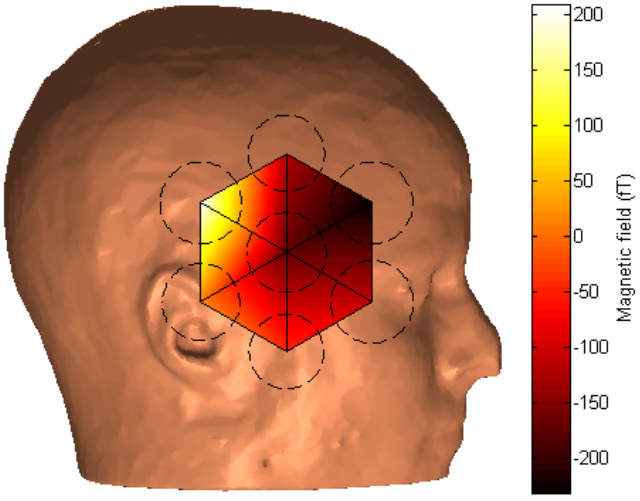

Fig. 4. Magnetic field map of the N100m response (peaks at 100 ms after stimulus on-set in Fig. 3) overlaid on the subject's scalp.

By using the field map in Fig. 4 a dipole model of the auditory response is fitted to the MEG data, as shown in the bottom right panel of Fig. 6. The dipole fit had a χ^2 of 0.93.

C. Ultra-low field MRI

Three MR slices from the ULF-MRI/MEG protocol are shown in Fig. 5. The three slices are separated by 6 mm each. The total ULF-MR/MEG imaging time was ~40 min, out of which 20 % of the time was pre-polarization time, and 65 % wait time in-between the MRI protocol and the auditory stimulus.

In Fig. 6 a total of 5 repetitions have been averaged to reduce the noise and consequently a fourth slice was obtained. The total imaging time was ~43 min. The ULF MR images are compared to their high-field counter-parts, which were obtained at the Mind Research Network [18] in their Siemens 3T Trio.

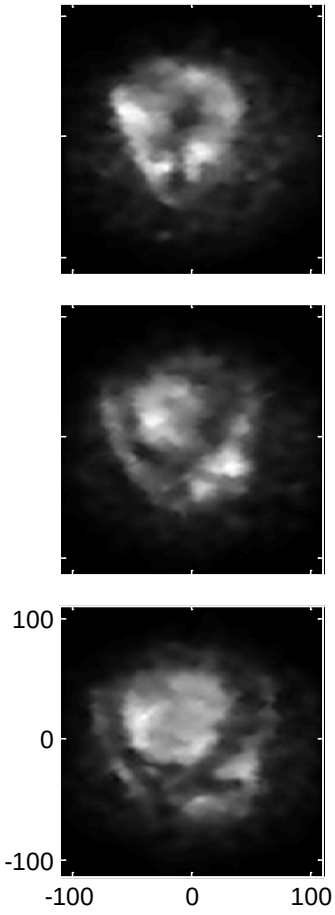

Fig. 5. Three slices from a single ULF-MRI/MEG run. The slices have a separation of 6 mm. The

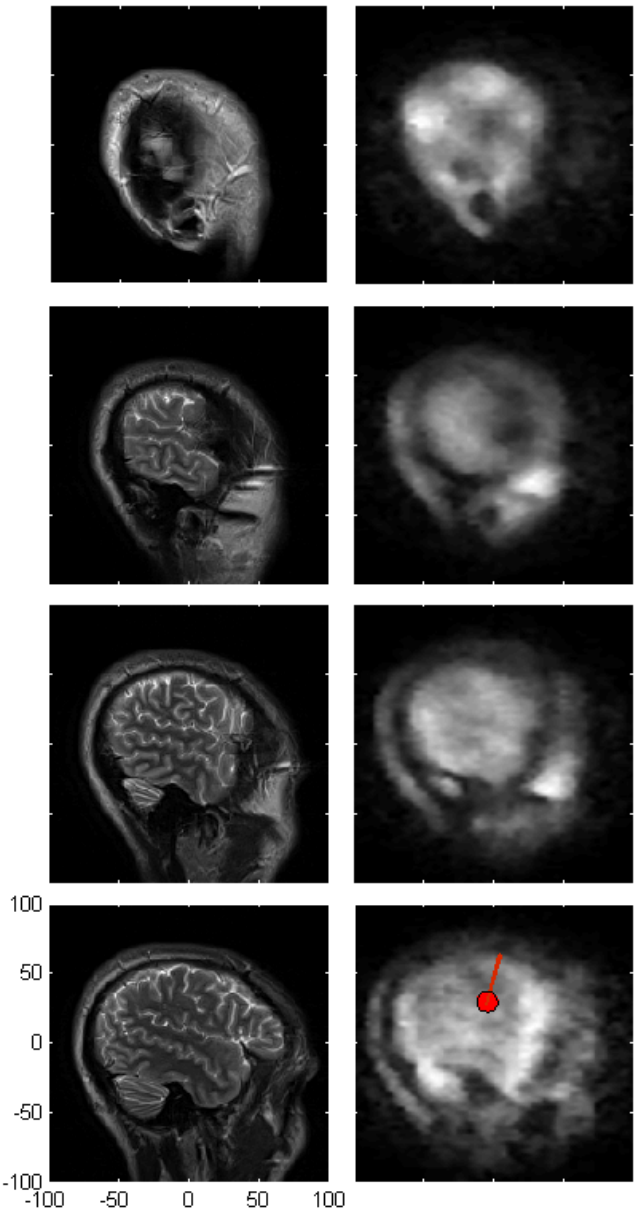

Fig. 6. High-field (left column) and ULF (right column) MR slices with axes in mm. The high-field slices were imaged in a 3 T system while the ULF slices were imaged at a 94 μT field. In the bottom right panel a dipole fit of the N100m field map (Fig. 4) is shown.

IV. Discussion

Co-registering the ULF MRI and the MEG with interleaved measurements provides a true mapping between the two modalities. By using small localization coils on, e.g., a swim-cap the location can be precisely mapped before and after the run. With a head motion-tracking system possible head movements could be detected in real-time.

A drawback of the interleaved measurement scheme is the necessary waiting time in-between the MRI protocol and the MEG measurement for each point in *k*-space. The wait time constitutes 65 % of each measurement point. The pulsed fields in the MRI protocol induce eddy-currents and magnetizes the walls of the magnetically shielded room [19]. The dominating transient fields inside the room come from the magnetization

of the μ-metal and from the eddy-currents in the μ-metal [19]. However, the time constant for the fields from the μ-metal is less than 1 ms, while the corresponding time constant for the aluminum is ~1 s [19].

The effect of the transients is shown in Fig. 7 where two different waiting times have been used. Time zero in the plots is at the end of the pre-polarization. The transient fields have to stay within the dynamic range of the SQUIDs during the whole MEG acquisition time.

To increase the resolution of the ULF MR images the signal-to-noise ratio has to be increased. The helium cryostat in the present system has higher noise than the state-of-the-art cryostats, which would give a noise reduction by about a factor ~2. Also, the pre-polarization field can be increased to provide a higher magnetization. However, by increasing the pre-polarization field the transients in the magnetically shielded room increase and as a result interleaved ULF MRI/MEG protocol could become impossible to perform.

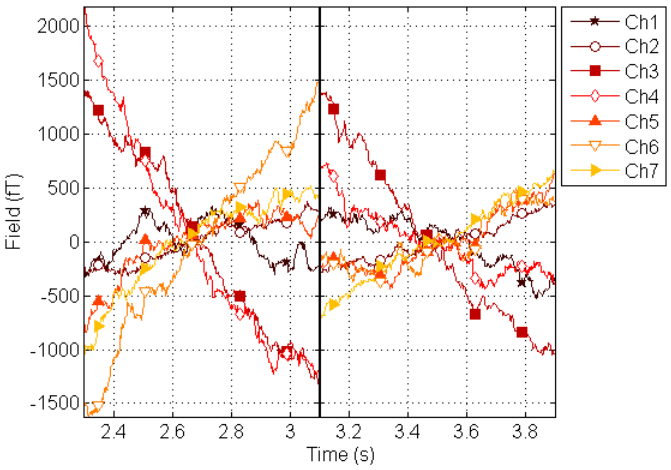

Fig. 7. SQUID signals after different waiting times after the MRI pulses. Displayed are averages of the individual channels from 18 epochs. No subject was present during these measurements.

In multi-modal imaging there have been reports of co-registration error as small as 1-2 mm [20]. In our system we observed a co-registration error of ~3 mm. Hence, further improvement is needed to achieve a smaller co-registration error in our present system.

V. Conclusion

We report on the first co-registered, interleaved ULF MRI and MEG measurements performed in our 7 channel low-T_c SQUID system. This work shows a proof-of-principle where both a functional MEG map and anatomical image slices are obtained in the same run. However, the imaging sequence contains a long waiting time between the MRI protocol and the auditory stimulus. Several separate images need to be averaged to provide contrast and to view deeper lying slices.

With stronger pre-polarization fields the transients will increase and interleaved ULF MRI and MEG measurements might become impossible. Separate measurements of the ULF MRI and the MEG in the same system might be necessary to keep the imaging time down.

References

[1] R. McDermott, and S. K. Lee, B. ten Haken, A. H. Trabesinger, A. Pines, and J. Clarke, "Microtesla MRI with a superconducting quantum interference device," *Proc. Natl. Acad. Sci. USA*, vol. 101. iss. 21, pp. 7857-7861, 2004.

[2] S. K. Lee, M. Mößle, W. Myers, N. Kelso, A. H. Trabesinger, A. Pines, and J. Clarke, "SQUID-detected MRI at 132 μT with *T*1-weighted contrast established at 10 μT-300 mT," *Magn. Reson. Med*., vol. 53, pp. 9-14, 2005.

[3] M. Mößle, S. I. Han. W. R. Myers, S. K. Lee, N. Kelso, M. Hatridge, A. Pines, and J. Clarke, "SQUID-detected microtesla MRI in the presence of metal," *J. Magn. Reson*. vol. 179, pp. 146-151, 2006.

[4] V. S. Zotev, A. N. Matlachov, P. L. Volegov, J. H. Sandin, M. A. Espy, J. C. Mosher, A. V. Urbaitis, S. G. Newman, and R. H. Kraus Jr., "Multi-channel SQUID system for MEG and ultra-low-field MRI," *IEEE Trans. Appl. Supercond.*, vol. 17, pp. 839-842, 2007.

[5] V. S. Zotev, P. L. Volegov, A. N. Matlashov, M. A. Espy, J. C. Mosher, and R. H. Kraus Jr., "Parallel MRI at microtesla fields," *J. Magn. Reson.*, vol. 192, pp. 197-208, 2008.

[6] V. S. Zotev, A. N. Matlashov, P. L. Volegov, I. M. Savukov, M. A. Espy, J. C. Mosher, J. J. Gomez, and R. H. Kraus Jr., "Microtesla MRI of the human brain combined with MEG," *J. Magn. Reson.*, vol. 194, pp. 115-120, 2008.

[7] R. H. Kraus Jr., P. Volegov, A. Matlachov, and M. Espy, "Toward direct neural current imaging by resonant mechanisms at ultra-low field," *NeuroImage*, vol. 39, pp. 310-317, 2008.

[8] M. Burghoff, H. H. Albrecht, S. Hartwig, I. Hilschenz, R. Körber, T. S. Thömmes, H. J. Scheer, J. Voigt, and L. Trahms, "SQUID system for MEG and low field magnetic resonance," *Metrol. Meas. Syst*., vol. XVI, pp. 371-375, 2009.

[9] M. Burghoff, H. H. Albrecht, S. Hartwig, I. Hilschenz, R. Körber, N. Höfner, H. J. Scheer, J. Voigt, L. Trahms, and G. Curio, "On the feasibility of neurocurrent imaging by low-field nuclear magnetic resonance," *Appl. Phys. Lett*., vol. 96, 233701, 2010.

[10] M. Espy, M. Flynn, J. Gomez, C. Hanson, R. Kraus, P. Magnelind, K. Maskaly, A. Matlashov, S. Newman, T. Owens, M. Peters, H. Sandin, I. Savukov, L. Schultz, A. Urbaitis, P. Volegov, and V. Zotev, "Ultra-low-field MRI for the detection of liquid explosives," *Supercond. Sci. Technol*., vol. 23, 034023, 2010.

[11] J. Nieminen, M. Burghoff, L. Trahms, and R. Ilmoniemi, "Enhancement of MRI by polarization encoding," *J. Magn. Reson*., vol. 202, pp. 211-213, 2010.

[12] J. Clarke, M. Hatridge, and M. Mößle, "SQUID-detected magnetic resonance imaging in microtesla fields," *Ann. Rev. Biomed. Eng.*, vol. 9, pp. 389-413, 2007.

[13] M. Packard and R. Varian, "Free nuclear induction in the Earth's magnetic field," *Phys. Rev*. vol. 93, p. 941, 1954.

[14] M. Hämäläinen, R. Hari, R. J. Ilmoniemi, J. Knuutila, O. V. Lounasmaa, "Magnetoencephalography—theory, instrumentation, and applications to noninvasive studies of the working human brain," *Rev. Mod. Phys*., vol. 65, pp. 413–497, 1993.

[15] Supracon AG, Jena, Germany, http://www.supracon.com

[16] NanoPore, Albuquerque, NM, USA, http://www.nanopore.com

[17] Polhemus, Colchester, VT, USA, http://www.polhemus.com

[18] Mind Research Network, Albuquerque, NM, USA, http://www.themindinstitute.org

[19] P. T. Vesanen, J. O. Nieminen, J. Dabek, and R. J. Ilmoniemi, "Hybrid MEG-MRI: geometry and time course of magnetic fields inside a magnetically shielded room," in *Proceedings of the 17th International Conference on Biomagnetism*, Dubrovnik, 2010, pp. 78-81.

[20] N. Hironaga, M. Schellens, and A. A. Ioannides, "Accurate co-registration for MEG reconstructions," in *Proceedings of the 13th International Conference on Biomagnetism*, Jena, 2002, pp. 931-933.